NANO LETTERS

pubs.acs.org/NanoLett Letter

Synergistic Fluid Minilaboratory Incorporating Femtosecond Laser-Engineered Heterogeneous Dual-Component

Shaojun Jiang, Qianqian Zhang, Dong Wu, Steven Wang,* Wei Li, Yiyu Chen, Juan Zhang, Ying Zhou, Cheng Peng,* Jiawen Li, Jiaru Chu, and Yanlei Hu*

Cite This: https://doi.org/10.1021/acs.nanolett.6c00074 Read Online

ACCESS | Metrics & More | Article Recommendations | Supporting Information

ABSTRACT: Miniaturized laboratories (mini-lab) centered on droplet/bubble-based microreactions hold immense promise for various applications. Magnetic excitation is widely utilized in open-surface minilaboratories, but the intrinsic properties of magnetic media limit mini-lab functionalization. Here we propose a mini-lab assembled from two femtosecond laser-engineered heterogeneous components, leveraging synergistic effects to extend functionality in droplet/bubble-based mini laboratories. The system comprises two distinct components, each capable of independent droplet/bubble manipulation: a magnetic superhydrophobic component integrating strong magnetic/photothermal properties (minimum driving magnetic field of ~12.7 mT), and a magnetic transparent component featuring superior transparency (transmittance of ~83.1%) for unimpeded visual access to the encapsulated liquid. The mini-lab is assembled from two components that not only combine their individual strengths but also generate additional functions through their synergy. It can effectively mitigate evaporation (~70.8%), prevent contamination, and move on various substrates. This synergy strategy endows the mini-lab with advantages for compact laboratory applications, demonstrating its versatile capabilities.

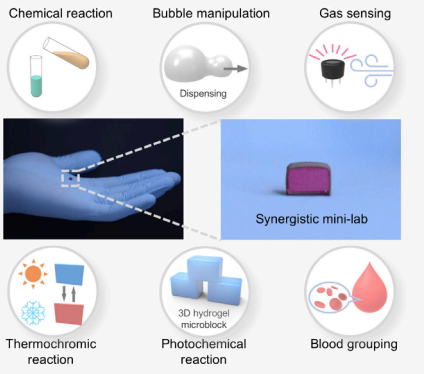

KEYWORDS: *droplet manipulation, miniaturized laboratories, synergistic, femtosecond laser, magnetic response*

Miniaturized laboratories (mini-lab) based on droplet and bubble systems are capable of efficiently performing both reaction and detection processes. Their remarkable flexibility, adaptability, versatility, and cost-effectiveness give them vast potential in the precision-engineered fields of biomedicine and fine chemistry.[1−4] On open surfaces, droplets or bubbles act as independent systems for microscale experiments, whose manipulation depends on external stimuli to realize controlled transport, merging, and mixing, along with optical or electrochemical detection.[5,6] Compared to acoustic, optical, and electrical stimuli, magnetic actuation provides a promising contactless approach with minimal latency.[5,7−9] Magnetic media can convert magnetic forces into driving forces for droplet/bubble manipulation. Common magnetic media primarily consist of magnetic additives and magnetically responsive elastomers. Magnetic additives, such as ferrofluids,[10,11] magnetic powders,[1,12] and magnetic beads,[13,14] are typically incorporated directly into the surface or interior of droplets/bubbles, where magnetic forces are transformed into interfacial forces to propel droplets or bubbles. In contrast, magnetically responsive elastomers embed magnetic additives within an elastomeric substrate, which undergoes controllable deformation under an external magnetic field, thereby directly driving the droplets or bubbles. Representative structures of magnetically responsive elastomeric substrates include magnetic micropillars,[15,16] microcones,[17,18] microplates[19,20] and micropits.[21,22] Magnetic additives offer flexible droplet/bubble manipulation capabilities, such as transport along nonfixed paths. However, they may contaminate the reagents and require subsequent purification steps.[10,23] In contrast, magnetically responsive substrates avoid contamination of reagents by additives, but exposed droplets on open surfaces are prone not only to evaporation but also to environmental contamination.[15,24]

Manipulation of droplets or bubbles using magnetic media enables the implementation of core functions such as reaction and detection in miniaturized laboratories.[1,10,21,25] Controlled reactions necessitate flexible and versatile manipulations, including transport, merging, and mixing. These capabilities depend on carefully designed structures as well as strong magnetic responsiveness, which in turn relies on a high proportion of magnetic additives.[26,27] In contrast, optical detection and photochemical reactions requires superior optical properties, which necessitates a reduced proportion of magnetic additives to ensure that light can directly penetrate

Received: January 6, 2026
Revised: April 16, 2026
Accepted: April 17, 2026

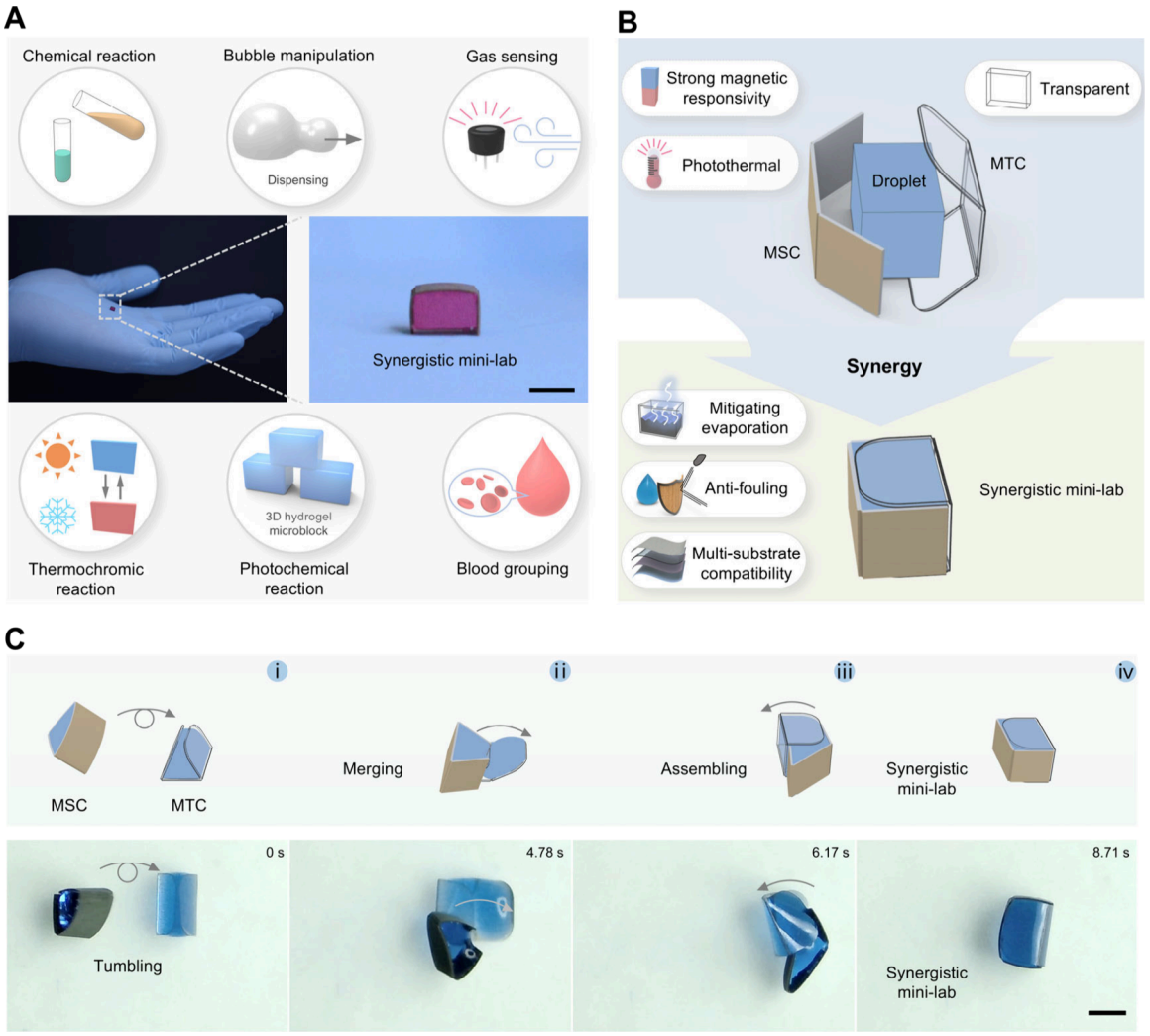

Figure 1. Synergistic fluid mini-lab for compact laboratory applications. (A) Optical images of the synergistic mini-lab. A synergistic mini-lab measuring 3 × 2 × 2 mm^3 can be applied in reagent mixing and reactions, bubble manipulation, gas sensing, thermochromic reactions, photochemical reactions, and blood grouping. Scale bar is 2 mm. (B) Schematic diagram of two heterogeneous components synergistically assembled into a mini-lab. The synergistic mini-lab integrates the respective advantages of its two components, combining the strong magnetic responsiveness and photothermal properties of MSC with the superior transparency of MTC. Moreover, through their synergistic interaction, additional functions are achieved, including the effective slowing of liquid evaporation, enhanced resistance to contamination, and improved compatibility with various substrates. (C) MSC and MTC assemble into a synergistic mini-lab. MSC carries the droplet to tumble toward the MTC. Two components assemble into a mini-lab under the action of magnetic fields and capillary force. Scale bar is 2 mm.

the encapsulating shell of the droplets or the substrate supporting the droplets.[28−31] There is an inherent trade-off between magnetic responsiveness and transparency, making it challenging for the magnetically responsive mini-lab system to simultaneously achieve strong magnetic performance and excellent optical properties.[29,32] This limitation hinders the ability to fulfill the diverse requirements of magnetically responsive minilaboratories, including flexible reagent manipulation (liquid and gas reagents), optical detection, and photochemical reactions.

Collaboration among diverse individuals often produces synergy beyond the sum of their parts. In nature, this synergy allows organisms to combine unique skills, increasing the success rate of tasks and enabling tasks impossible alone. For example, groupers and giant moray eels use complementary cooperative hunting strategies—groupers hunt in open water, while moray eels hunt in reefs—making prey inescapable and increasing their success. Similarly, weaver ants cooperate to build large nests, with adult ants collectively shaping the leaves and larvae secreting silk to secure the nest structure.[33,34] These provide an effective solution for enhancing the performance and expanding the functionality of magnetically responsive mini laboratories. Unlike traditional methods that typically enhance one property at the expense of another, we draw inspiration from animal synergistic behaviors and propose a synergistic fluidic mini-lab. It is assembled from two femtosecond laser-engineered heterogeneous components to achieve the coexistence of strong magnetic responsiveness and excellent optical transparency, thereby enhancing the mini-lab's capabilities in controlled reactions and detection. The magnetic superhydrophobic component (MSC), containing a high concentration of magnetic particles, exhibits strong magnetic responsiveness (minimum driving magnetic field of ~12.7 mT) along with excellent photothermal performance, enabling flexible manipulation of fluids as well as remote heating. The magnetic transparent component (MTC)

https://doi.org/10.1021/acs.nanolett.6c00074
Nano Lett. XXXX, XXX, XXX−XXX

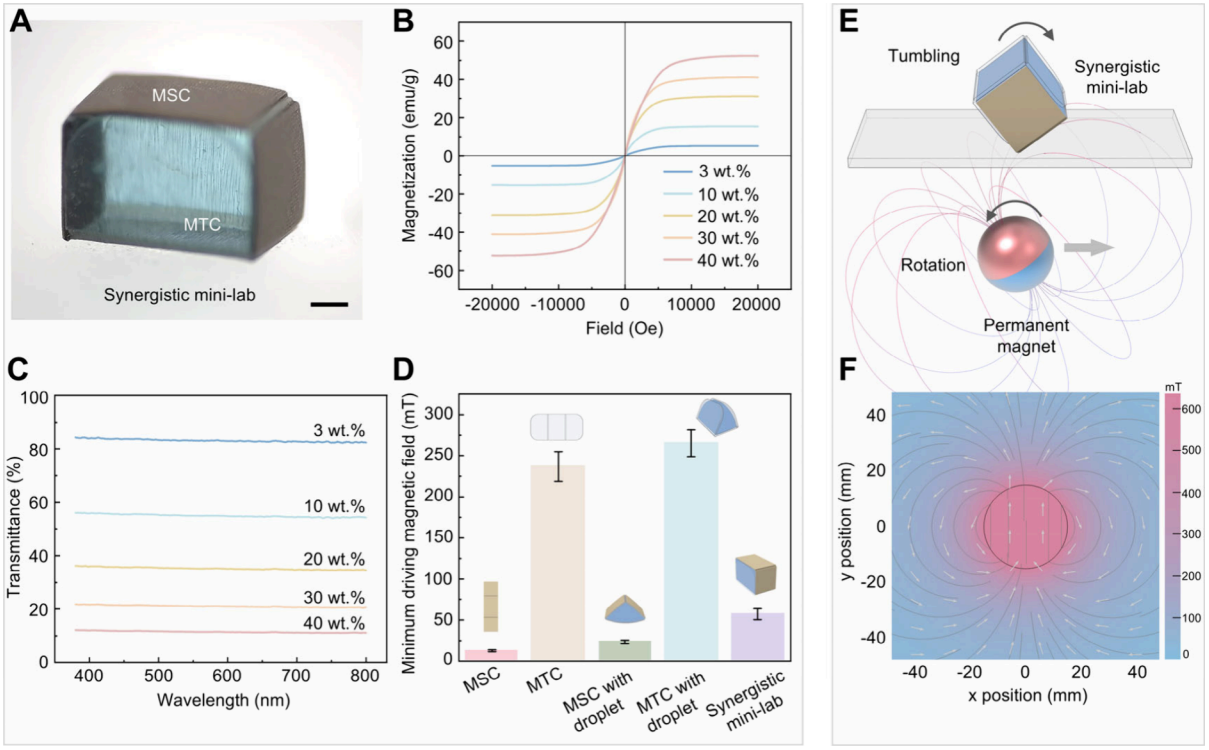

Figure 2. Magnetic responsiveness of the synergistic mini-lab. (A) Optical image of the synergistic mini-lab. Scale bar is 500 μm. (B) Magnetization of PDMS films with different iron particle contents. (C) Transmittance of PDMS films with different iron particle contents. (D) The minimum driving magnetic fields for MSC, MTC, MSC with droplet, MTC with droplet and synergistic mini-lab, respectively. (E) Schematic diagram of the driving system. A spherical permanent magnet generates a periodically varying magnetic field through rotation, driving the synergistic mini-lab to move directionally. (F) Magnetic field simulation of the spherical magnet.

minimizes the content of magnetic particles while ensuring effective magnetic responsiveness, thereby achieving an excellent optical performance (transmittance of ~83.1%). This enhances optical accessibility, enabling direct optical observation of internal liquids or facilitating photochemical reactions. All of them can independently manipulate both droplets and bubbles. Notably, the strong magnetic responsiveness and superhydrophobic nature of the MSC enable flexible bubble splitting and release, surpassing other strategies that are limited to simple bubble transport and merging.[11,17,18,35] The synergistic mini-lab not only harmoniously integrates the individual advantages of each component but also demonstrates additional functionalities arising from their synergy. For instance, it effectively suppresses liquid evaporation (~70.8%), prevents external contamination, and reduces substrate dependence, thereby enabling controlled manipulation of liquids on surfaces with varying wettability (even a superhydrophilic substrate). These characteristics are crucial for microreaction systems,[36,37] enabling the synergistic mini-lab to demonstrate significant advantages in compact laboratory applications.

The synergistic fluid mini-lab demonstrates flexible fluid manipulation capability and diverse functionalities, offering attractive advantages in compact laboratory applications. As illustrated in Figure 1A, we have developed a synergistic mini-lab with dimensions of 3 × 2 × 2 mm^3, capable of accommodating liquid or gas (12 μL), thereby enabling flexible reaction and detection processes across diverse fields such as fine chemistry and biomedical. Specifically, we demonstrate its applications in reagent mixing and reactions, bubble manipulation, gas sensing, thermochromic reactions, photochemical reactions, and blood grouping. As shown in Figure 1B, the synergistic mini-lab is assembled from MSC and MTC driven by capillary forces. Both MSC and MTC are fabricated via femtosecond laser processing of Polydimethylsiloxane (PDMS) films doped with iron particles (Figure S1). Owing to the high concentration of iron particles in MSC, it demonstrates both strong magnetic responsiveness and significant photothermal effects. In contrast, MTC contains a smaller amount of iron particles, resulting in relatively weaker magnetic responsiveness but enhanced optical performance. The difference in iron particle concentration leads to the magnetic and optical heterogeneity between MSC and MTC. The synergy between the two heterogeneous components enables the mini-lab to not only efficiently integrate the individual properties of both components but also confer additional advantages. In particular, the synergistic mini-lab combines the strong magnetic responsiveness and photothermal characteristics of MSC with the transparent optical window formed by MTC. Moreover, their synergistic interaction effectively slows liquid evaporation, enhances antifouling performance, and enables compatibility with various substrates. The assembly process of the synergistic mini-lab is illustrated in Figure 1C (Movie S1). MSC and MTC can each independently load droplets (6 μL). The significant difference in magnetic responsivity (>200 mT) allows the MTC to remain stationary while the MSC is being manipulated, instead of being driven simultaneously. Upon contact, increasing the magnetic field intensity triggers the MTC to unfold and expose its encapsulated droplet, while the MSC deforms, allowing their loaded droplets to merge. By regulating the assembly with magnetic field, two components

https://doi.org/10.1021/acs.nanolett.6c00074
Nano Lett. XXXX, XXX, XXX−XXX

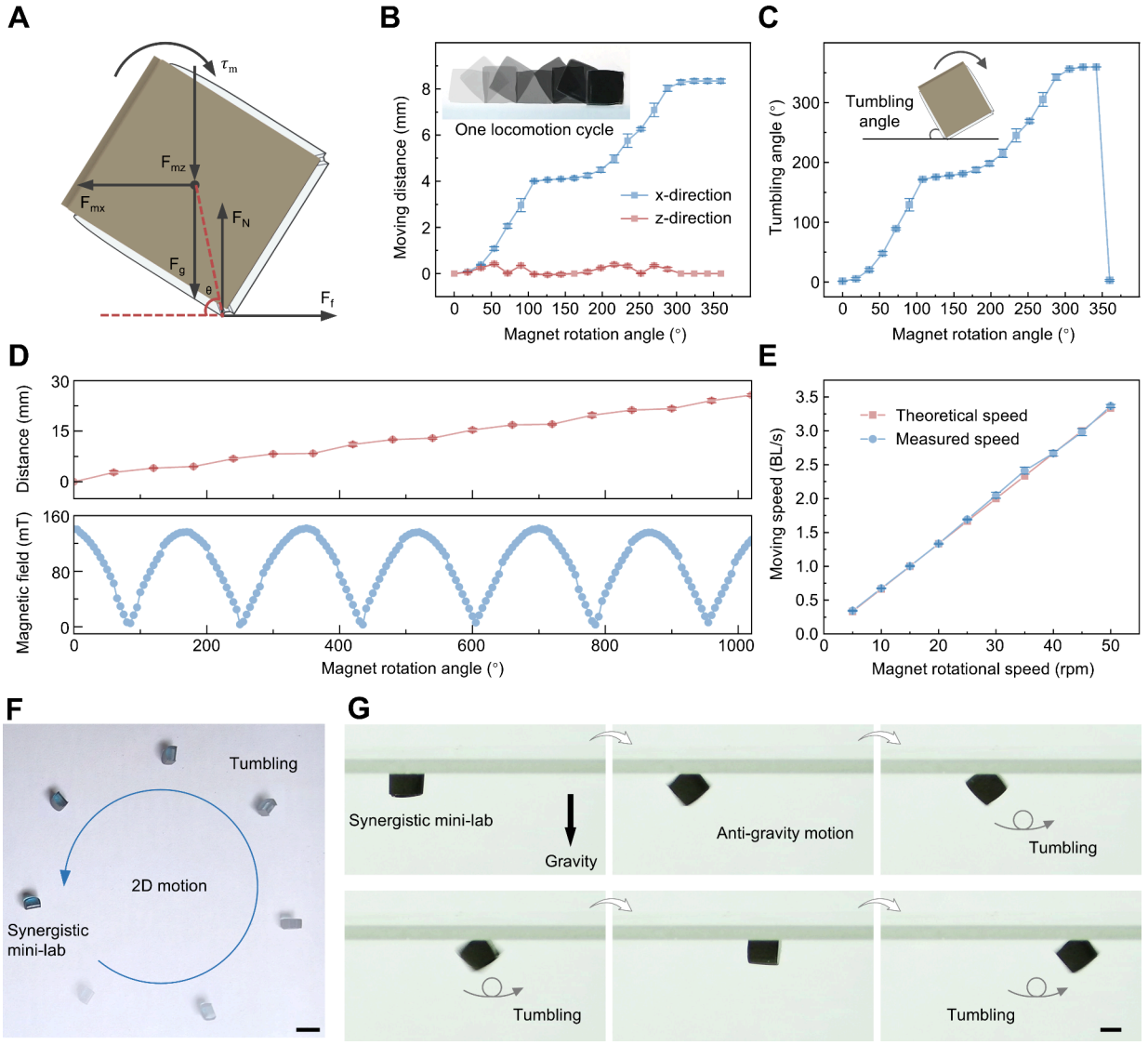

Figure 3. Motion performance of the synergistic mini-lab. (A) Schematic diagram of forces acting on the synergistic mini-lab during tumbling. The mini-lab experiences gravitational force F_g, vertical magnetic force component F_{mz}, and supporting force F_N in the vertical direction. In the horizontal direction, it is subjected to horizontal magnetic force component F_{mx}, and frictional force F_f. Additionally, the mini-lab is influenced by a magnetic torque τ_m. (B) Relationship between the displacement of the synergistic mini-lab and the rotation angle of the magnet. The inset shows one tumbling cycle of the synergistic mini-lab. (C) Relationship between the tumbling angle of the synergistic mini-lab and the rotation angle of the magnet. The inset is the schematic diagram of the tumbling angle. (D) Relationship between the magnetic field intensity, the displacement of the synergistic mini-lab, and the rotation angle of the magnet during the continuous movement of the synergistic mini-lab. (E) Relationship between the moving speed of the synergistic mini-lab and the rotation speed of the magnet. (F) The synergistic mini-lab moves in a 2D plane. Scale bar is 5 mm. (G) The synergistic mini-lab resists gravity to transport a water droplet on an inverted surface. Scale bar is 2 mm.

can assemble into the mini-lab with the assistant of the capillary force.[38,39]

MSC and MTC stably assemble into a synergistic mini-lab that maintains strong magnetic actuation performance while featuring a broad transparent optical window, significantly enhancing optical accessibility and enabling applications such as optical monitoring and photochemical reactions (Figure 2A). These advantages of the synergistic mini-lab enable it to meet the demands of controllable reactions, real-time monitoring, and product analysis in microreaction processes. Notably, these processes impose stringent requirements on both the magnetic responsiveness and optical properties of the device, which existing systems based on a single magnetic medium struggle to meet due to the inherent challenge of simultaneously enhancing both performance aspects.[10,16,21,29,31,32,40] Figures 2B and 2C clearly illustrate the interrelation between the magnetic responsiveness and optical properties of an individual magnetic medium. A series of magnetic PDMS films with varying iron particle concentrations are prepared and systematically tested. As shown in Figure 2B, the magnetic responsiveness of the films significantly increases as the iron concentration rises from 3 to 40 wt %. However, their transmittance decreases from ~83.1% to ~11.5%, as illustrated in Figure 2C. Based on these results, magnetic films containing 40 wt % iron particles are selected to ensure strong magnetic responsiveness, while films with 3 wt % iron particles are chosen to maximize optical transparency while ensuring sufficient magnetic drivability. These two selected films are subsequently processed into the component structure via femtosecond laser direct writing (Figure S1). This process

https://doi.org/10.1021/acs.nanolett.6c00074
Nano Lett. XXXX, XXX, XXX−XXX

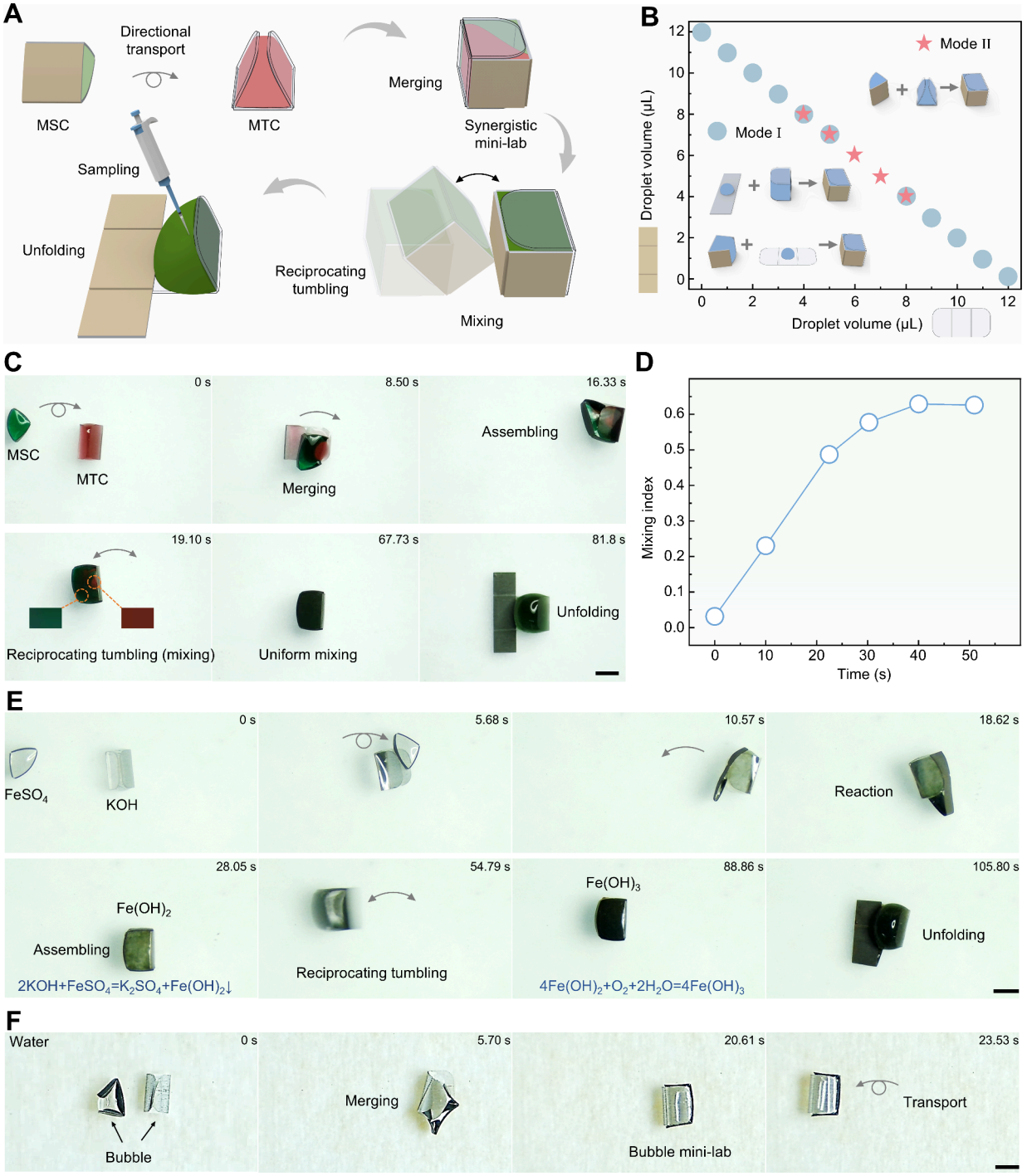

Figure 4. Fluid manipulation performance of the synergistic mini-lab. (A) Schematic diagram of the synergistic mini-lab for liquid merging and mixing. The mini-lab achieves rapid mixing of liquids through reciprocal tumbling and can then unfold for subsequent sampling. (B) Assembly modes of two components with different droplet volume distributions. The total volume of the droplet keeps at 12 μL. (C) Synergistic mini-lab for efficient liquid mixing. The two components are loaded with green and red 50% glycerol solutions, respectively, and are magnetically assembled into a synergistic mini-lab. The mini-lab mixes the solutions by reciprocal tumbling and then unfolds for further operations. (D) Mixing index of the solution during the reciprocal tumbling of the synergistic mini-lab. (E) Synergistic mini-lab for chemical cascade reactions. Two components are loaded with $FeSO_4$ droplet and KOH droplet, respectively, and assembled into the mini-lab to merge the droplets for reaction to form the $Fe(OH)_2$. The synergistic mini-lab further oxidized $Fe(OH)_2$ to form $Fe(OH)_3$ by reciprocating tumbling. (F) Two components assemble into a synergistic bubble mini-lab. All scale bars are 2 mm.

induces surface ablation and micro/nanoparticle deposition on the magnetic film. By controlling the processing parameters, we can achieve both contour cutting of the components and on-demand construction of micro/nanostructures for tailoring surface wettability, thereby imparting distinct surface characteristics to the two components (Figure S2). We optimized the morphology (including the rectangular contours of MSC and MTC as well as the rounded edges of MTC), surface wettability (with one side of MSC modified to be superhydrophobic), motion modes, and assembly modes of the two

https://doi.org/10.1021/acs.nanolett.6c00074
Nano Lett. XXXX, XXX, XXX−XXX

components to ensure stable assembly of the synergistic mini-lab while maximizing the transparent optical window (Figures S2−S12). The minimum magnetic field strengths required to drive different components are shown in Figure 2D. Notably, the synergistic mini-lab can be actuated by a relatively low magnetic field strength (~57 mT). The schematic of the driving system for the synergistic mini-lab is shown in Figure 2E. A rotating spherical magnet produces a periodically varying magnetic field that propels the mini-lab to tumble directionally. The corresponding magnetic field simulation is presented in Figure 2F, while the magnetic flux density is detailed in Figure S13, Supporting Information.

Within the rotating magnetic field, the synergistic mini-lab experiences both magnetic force (F_m) and magnetic torque (τ_m), which can be described as follows (Figure 3A, Supplementary Note 1):[41,42]

$$\mathbf{F}_m = NV(\mathbf{M}\cdot\nabla)\mathbf{B} \quad (1)$$

$$\boldsymbol{\tau}_m = NV(\mathbf{M}\times\mathbf{B}) \quad (2)$$

where N is the total number of iron particles contained within the synergistic mini-lab, V is the volume of an iron particle, M is the magnetization of the iron particle, B is the magnetic flux density of the spherical magnet. A full rotation of the magnet drives the synergistic mini-lab to complete one tumbling cycle. The relationships between the rotation angle of the magnet and the displacement of the synergistic mini-lab in the xz-plane, as well as its tumbling angle, are presented in Figures 3B and 3C, respectively. As the rotation angle of the magnet increases, the tumbling angle of the mini-lab correspondingly grows, resulting in a net displacement along the x-direction. One locomotion cycle of the synergistic mini-lab (i.e., one full tumble) corresponds to a displacement of approximately four body lengths (BL, ~8.3 mm). The continuous rotation of the magnet generates a periodically varying magnetic field, which drives the synergistic mini-lab to perform sustained tumbling motion (Figure 3D, Movie S2). The locomotion speed of the synergistic mini-lab (V) can be readily controlled by adjusting the rotation speed of the magnet (Figure 3E). It can be given by

$$V = \frac{4nBL}{60} \quad (3)$$

where n is the rotation speed of the magnet (rpm), BL is the body length of the synergistic mini-lab. With its excellent magnetic responsiveness, the synergistic mini-lab demonstrates remarkable locomotion capabilities. By precisely controlling the motion trajectory of the rotating magnet, programmable two-dimensional (2D) locomotion of the synergistic mini-lab can be achieved (Figure 3F). It is even capable of antigravity manipulation, such as tumbling forward on an inverted surface (Figure 3G, Movie S3).

The transport, merging, mixing, and sampling of reaction reagents are fundamental operations in droplet-based miniaturized laboratories. Through controlled assembly of its two components, the synergistic mini-lab can conveniently perform these functions. As shown in Figure 4A, leveraging the significant difference in magnetic responsiveness, the MSC can actively carry the reagent to approach the MTC. Under the influence of the magnetic field, the two components undergo deformation, facilitating the merging of internal liquids. Through flexible magnetic manipulation, the dual-component system can be assembled into the synergistic mini-lab. Upon assembly completion, this mini-lab achieves rapid reagent mixing through a reciprocal tumbling motion, thereby facilitating the reaction process. After the reaction finishes, the synergistic mini-lab can unfold to allow for sampling and other subsequent operations. The detailed unfolding and sampling processes are illustrated in Figure S14. Under magnetic modulation, the system enables reversible switching between the unfolded and wrapped states, allowing repeated sampling without additional steps and thus avoiding sample loss or contamination (Figures S15 and S16 and Movie S4). Moreover, the intrinsic hydrophobicity of PDMS ensures minimal residue during sample retrieval from the unfolded synergistic mini-lab (Figure S17). Depending on the volume of the carried reagents, the synergistic mini-lab can be assembled in different modes (Figure 4B). In mode I, one component carries a small droplet and remains unfolded during the assembly process, while the other component is in a wrapped (folded) state. In mode II, both components are loaded with droplets within the appropriate volume range and they both transition into a folded state during the assembly process (Figure S18).

The synergistic mini-lab for efficient liquid mixing is illustrated in Figure 4C. The MSC and MTC are, respectively, loaded with green and red aqueous glycerol solutions (50% v/v). Initially, the MSC moves toward and contacts the MTC. Then, as the magnetic field intensifies, both components deform, allowing the encapsulated liquids to come into contact. The two components bind through capillary forces, followed by magnetically controlled tumbling to fine-tune the assembly, ultimately forming a well-defined rectangular structure (i.e., synergistic mini-lab). During the assembly process, some liquids begin to mix, although delamination still persists. By regulating the reciprocating tumbling of the synergistic mini-lab, the glycerol solutions are uniformly mixed. The resulting reagents can then be sampled on demand by controlling the unfolding of the mini-lab (Movie S5). The entire mixing procedure is observable through the optical window formed by the MTC. As shown in Figure 4D, effective mixing of the liquids can be achieved in approximately 50 s. The same process is likewise applicable to chemical cascade reactions (Figure 4E, Movie S6). The ferrous sulfate solution ($FeSO_4$, 0.25 mol·L^{-1}, 6 μL) and potassium hydroxide solution (KOH, 0.5 mol·L^{-1}, 6 μL) are loaded by MSC and MTC, respectively. The assembly facilitates the reaction between the two solutions, culminating in the precipitation of a white ferrous hydroxide precipitate ($Fe(OH)_2$). The reciprocating tumbling of the synergistic mini-lab allows the $Fe(OH)_2$ to be further oxidized to produce green ferric hydroxide ($Fe(OH)_3$). The reaction product is obtainable by unfolding the synergistic mini-lab. By observation of the color changes of the reactants through the optical window, the advancement of the reaction can be evaluated. In addition, through the cooperative assembly of the two components, the synergistic mini-lab is employed to construct three-dimensional hydrogel microblocks, providing a platform for engineered tissue applications[43] (Figure S19). Importantly, the design of the synergistic mini-lab ensures robust scalability, allowing it to be adapted for use in small-volume droplet systems without compromising its functional performance (down to 2 μL, Figure S20). Besides liquids, gases are another commonly encountered reactive substance. The bubble-based microreactions demonstrate remarkable promise within the realms of gas analysis and detection applications.[6,44] The synergistic mini-lab is also

https://doi.org/10.1021/acs.nanolett.6c00074
Nano Lett. XXXX, XXX, XXX−XXX

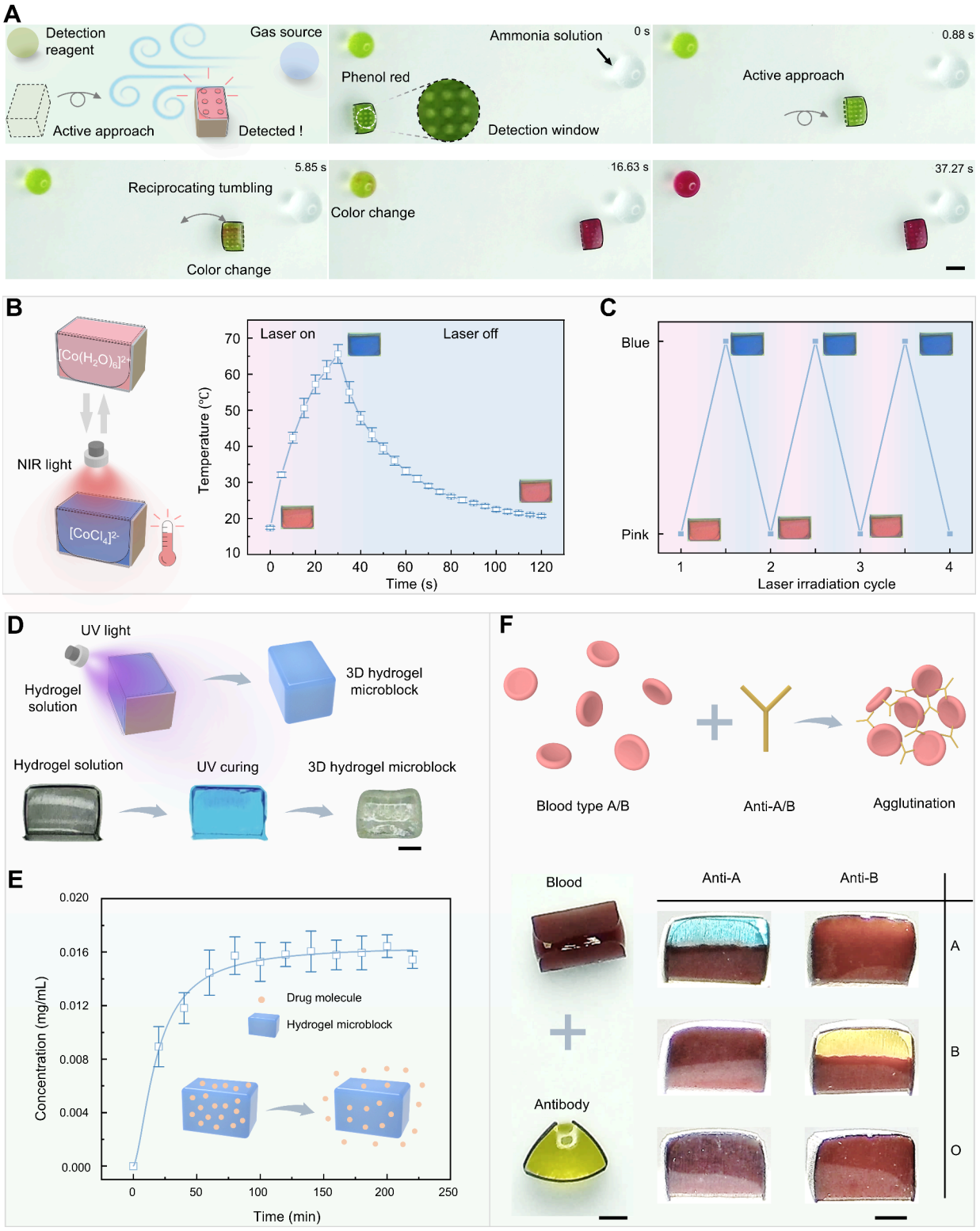

Figure 5. Diverse compact laboratory applications based on the synergistic mini-lab. (A) Synergistic mini-lab for gas sensing. The synergistic mini-lab loads detection reagent and actively approaches the gas source. It reciprocates to enable rapid gas sensing. Scale bar is 2 mm. (B) Remote heating of the synergistic mini-lab via photothermal effect for thermochromic reaction. The temperature−time curve demonstrates that as NIR laser irradiation is applied, the temperature of the synergistic mini-lab gradually increases. The insets show the color of the internal solution changing from blue to pink. (C) Reversible heating of the synergistic mini-lab. (D) Synergistic mini-lab enables UV curing of 3D hydrogel microblocks through the optical window. Scale bar is 1 mm. (E) The hydrogel microblocks is used for sustained drug release. (F) Synergistic mini-lab is used as a biomedical microreactor to enable blood grouping. Scale bars are 1 mm.

applicable to bubble systems without the need for additional surface modification. As shown in Figure 4F, the two components can be individually loaded with air bubbles (6 μL). The MSC carries the bubble to actively approach the

https://doi.org/10.1021/acs.nanolett.6c00074
Nano Lett. XXXX, XXX, XXX−XXX

MTC. Upon contact, both components are controlled to deform by increasing the magnetic field, leading to the merging of the wrapped bubbles. Through the combined effects of capillary forces and magnetic fields, the two components assemble into a synergistic bubble mini-lab, which enables flexible manipulation of gas samples (Movie S7). Beyond bubble transport and merging, the MSC achieves controlled splitting and on-demand release of microbubbles by utilizing its superhydrophobic surface and flexible magnetically responsive manipulation capabilities (Figure S21). This capability is essential for achieving diverse and flexible manipulations in bubble-based microreactions, yet it poses a significant challenge to existing magnetically responsive strategies that are limited to bubble transport and merging.[11,17,18,45]

Leveraging synergistic effects, the mini-lab achieves enhanced performance and expanded functionality, offering significant advantages for compact laboratory applications. The transparent window formed by the MTC enables direct optical observation and facilitates photochemical reactions, thereby enhancing its utility in microchemistry and biomedicine.[46] Combined with the exceptional magnetic manipulability provided by the MSC, the synergistic mini-lab demonstrates distinct capabilities for rapid gas sensing. As shown in Figure 5A, the synergistic mini-lab carrying detection reagent (phenol red, 12 μL) actively approaches the gas source (ammonia solution, 0.66%, 20 μL). A regular microporous array is constructed on the MTC as the detection window to enhance the contact area between the detection liquid and the gas (Figure S22). Moreover, the synergistic mini-lab is reciprocated near the gas source to enhance the interaction between the gas and the detection reagent, thereby improving the detection efficiency. The detection reagent inside the synergistic mini-lab undergoes a color change at 5.85 s, while the stationary detection reagent (12 μL) shows a color change at 16.63 s, by which time the synergistic mini-lab has turned completely red. The stationary detection reagent fully turned red at approximately 37.27 s (Movie S8). The strong photothermal effect from the high iron particles content in the MSC, combined with the optical window of the MTC, endows the synergistic mini-lab with distinctive application prospects in temperature-dependent microreactions. As shown in Figure 5B, a solution of cobalt chloride ($CoCl_2$) in hydrochloric acid (12 μL) is loaded in the synergistic mini-lab. The cobalt ions in solution at equilibrium are present in $CoCl_4^{2-}$ and $Co(H_2O)_6^{2+}$, that is $Co(H_2O)_6^{2+} + 4Cl^- \rightleftarrows CoCl_4^{2-} + 6H_2O$.[47] Initially, the solution appeared pink ($Co(H_2O)_6^{2+}$). When the near-infrared (NIR) laser is irradiated onto the mini-lab, the iron particles inside the components absorb the NIR light to generate heat, causing the equilibrium shift toward the blue $CoCl_4^{2-}$. The temperature increases form 17.4 ± 0.4 °C to 65.6 ± 2.6 °C after 30 s of irradiation. After the NIR light is removed, the temperature gradually decreases and the equilibrium shifts toward the pink $Co(H_2O)_6^{2+}$ again. The performance of reversible remoting heating is verified in cycle tests (Figure 5C, Movie S9). A control group experiment showed that the $CoCl_2$ solution does not undergo a color change when exposed to NIR light alone (Figure S23).

Leveraging the synergy of the two components' excellent magnetic and optical properties, the mini-lab also demonstrates great potential for biomedical applications. Figure 5D and 5E demonstrate the utilization of synergistic mini-lab for the fabrication of 3D hydrogel microblocks, which commonly serve as carriers for therapeutic agents, providing spatial and temporal control over their release.[48] As illustrated in Figure 5D, the hydrogel solution is initially loaded into the synergistic mini-lab. Beyond facilitating visual observation, the optical window also functions as a channel for photochemical reactions. Through this window, ultraviolet (UV) light directly irradiates the hydrogel solution, initiating cross-linking and leading to the formation of a 3D hydrogel microblock. Drug is preloaded into the hydrogel microblock to enable controlled release profiles. As shown in Figure 5E, the drug release concentration gradually increases over time, exhibiting effective temporal control. In addition, with its contactless operation and optical window, the synergistic mini-lab readily lends itself to rapid blood grouping applications. When the red blood cells exposed to the corresponding antibodies, they will produce a coagulation reaction.[49] As demonstrated in Figure 5F, two components are used to load blood and antibody, respectively. By collaborative assembly of two components, the blood and antibodies are thoroughly mixed (Figure S24). The distinct stratification of the condensed samples (anti-A + blood type A, anti-B + blood type B) can be visually observed through the optical window, with the upper portion displaying the color of antibodies and the lower part showcasing the condensed red blood cells. In other instances, the mixture remains uniformly deep red. Better optical transparency is more favorable for photochemical reactions or detection. It is encouraging that the MSC can also cooperatively assemble with transparent PDMS film (without iron particles doping) to form a synergistic mini-lab for more demanding applications (Figure S25). In addition to their individual advantages, the two components confer additional functionalities to the mini-lab through synergistic effects. For example, the mini-lab can effectively protect the internal liquid, slowing down its evaporation (~70.8%) while preventing contamination from the external environment. Moreover, the mini-lab demonstrates enhanced adaptability by reducing its dependence on substrate wettability, enabling the controlled transport of liquids across substrates with varying wettability, including superhydrophilic surfaces (Figures S26−S28). These features are of great significance for applications such as open-surface droplet microfluidic systems and microreactors.

In summary, we demonstrate a miniaturized fluid laboratory based on the synergy of two components targeting a wide range of droplet- and bubble-based compact laboratory applications. The synergistic mini-lab is assembled from two femtosecond laser-engineered magnetic components that each possess unique advantages and can independently manipulate droplets and bubbles. The MSC excels with its strong magnetic responsivity and photothermal properties, while the MTC is characterized by its high transparency. The rational magneto-responsive design and structural optimization of the components enable them to assemble rapidly and robustly into a synergistic mini-lab. This strategy not only fully leverages the advantages of both components but also generates additional benefits through synergistic effects. It is capable of mitigating liquid evaporation, avoiding potential contamination, and making the synergistic mini-lab suitable for multiple substrates. These features endow the mini-lab with significant advantages in compact laboratory applications that integrate controllable reactions and detection. The mini-lab enables flexible manipulation of droplets and bubbles, supports optical detection and photochemical reactions, and allows for

https://doi.org/10.1021/acs.nanolett.6c00074
Nano Lett. XXXX, XXX, XXX−XXX

remote heating. This represents a remarkable advancement over previous magnetically responsive droplet/bubble-based miniaturized laboratories, which had limited functionality and were difficult to expand. Empowered by this synergy, diverse miniaturized laboratory operations have been realized, thus holding significant importance for various fields, including fine chemistry, medical diagnostics, and other related disciplines.

■ ASSOCIATED CONTENT

Data Availability Statement

All data are available in the main text or the Supporting Information.

Supporting Information

The Supporting Information is available free of charge at https://pubs.acs.org/doi/10.1021/acs.nanolett.6c00074.

Additional experimental details, characterization, and analysis details (PDF)

Two components assemble into a synergistic mini-lab (MP4)

Directional tumbling of the synergistic mini-lab (MP4)

Two-dimensional and antigravity locomotion of the synergistic mini-lab (MP4)

Reversible unfolding and wrapping of the synergistic mini-lab (MP4)

Synergistic mini-lab for efficient liquid mixing (MP4)

Synergistic mini-lab for chemical cascade reactions (MP4)

Two components assemble into a synergistic bubble mini-lab (MP4)

Synergistic mini-lab for gas sensing (MP4)

Synergistic mini-lab for thermochromic reaction (MP4)

■ AUTHOR INFORMATION

Corresponding Authors

Steven Wang − *Department of Mechanical Engineering, City University of Hong Kong, Hong Kong 999077, China*; Email: steven.wang@cityu.edu.hk

Cheng Peng − *Department of Obstetrics and Gynecology, The First Affiliated Hospital of USTC, Division of Life Sciences and Medicine, University of Science and Technology of China, Hefei, Anhui 230001, China*; Email: gynpeng@ustc.edu.cn

Yanlei Hu − *Department of Obstetrics and Gynecology, The First Affiliated Hospital of USTC, Division of Life Sciences and Medicine, University of Science and Technology of China, Hefei, Anhui 230001, China; CAS Key Laboratory of Mechanical Behavior and Design of Materials, Key Laboratory of Precision Scientific Instrumentation of Anhui Higher Education Institutes, Department of Precision Machinery and Precision Instrumentation, University of Science and Technology of China, Hefei, Anhui 230027, China*; orcid.org/0000-0003-1964-0043; Email: huyl@ustc.edu.cn

Authors

Shaojun Jiang − *Department of Obstetrics and Gynecology, The First Affiliated Hospital of USTC, Division of Life Sciences and Medicine, University of Science and Technology of China, Hefei, Anhui 230001, China; CAS Key Laboratory of Mechanical Behavior and Design of Materials, Key Laboratory of Precision Scientific Instrumentation of Anhui Higher Education Institutes, Department of Precision Machinery and Precision Instrumentation, University of Science and Technology of China, Hefei, Anhui 230027, China; Department of Mechanical Engineering, City University of Hong Kong, Hong Kong 999077, China*; orcid.org/0000-0002-1429-4236

Qianqian Zhang − *CAS Key Laboratory of Mechanical Behavior and Design of Materials, Key Laboratory of Precision Scientific Instrumentation of Anhui Higher Education Institutes, Department of Precision Machinery and Precision Instrumentation, University of Science and Technology of China, Hefei, Anhui 230027, China*

Dong Wu − *CAS Key Laboratory of Mechanical Behavior and Design of Materials, Key Laboratory of Precision Scientific Instrumentation of Anhui Higher Education Institutes, Department of Precision Machinery and Precision Instrumentation, University of Science and Technology of China, Hefei, Anhui 230027, China*; orcid.org/0000-0003-0623-1515

Wei Li − *Interdisciplinary Research Center, School of Mechanical Engineering, Shanghai Jiao Tong University, Shanghai 200240, China*

Yiyu Chen − *CAS Key Laboratory of Mechanical Behavior and Design of Materials, Key Laboratory of Precision Scientific Instrumentation of Anhui Higher Education Institutes, Department of Precision Machinery and Precision Instrumentation, University of Science and Technology of China, Hefei, Anhui 230027, China*

Juan Zhang − *CAS Key Laboratory of Mechanical Behavior and Design of Materials, Key Laboratory of Precision Scientific Instrumentation of Anhui Higher Education Institutes, Department of Precision Machinery and Precision Instrumentation, University of Science and Technology of China, Hefei, Anhui 230027, China*

Ying Zhou − *Department of Obstetrics and Gynecology, The First Affiliated Hospital of USTC, Division of Life Sciences and Medicine, University of Science and Technology of China, Hefei, Anhui 230001, China*

Jiawen Li − *CAS Key Laboratory of Mechanical Behavior and Design of Materials, Key Laboratory of Precision Scientific Instrumentation of Anhui Higher Education Institutes, Department of Precision Machinery and Precision Instrumentation, University of Science and Technology of China, Hefei, Anhui 230027, China*; orcid.org/0000-0003-3950-6212

Jiaru Chu − *CAS Key Laboratory of Mechanical Behavior and Design of Materials, Key Laboratory of Precision Scientific Instrumentation of Anhui Higher Education Institutes, Department of Precision Machinery and Precision Instrumentation, University of Science and Technology of China, Hefei, Anhui 230027, China*; orcid.org/0000-0001-6472-8103

Complete contact information is available at: https://pubs.acs.org/10.1021/acs.nanolett.6c00074

Author Contributions

S.J. and Y.H. conceived the concept and designed the project. S.J., Q.Z., W.L., Y.C. and J.Z. produced samples. W.L., Y.C., J.Z. and C.P. assisted in the experimental apparatus. S.J., Q.Z., J.Z., and C.P. performed the characterization. S.J., D.W., S.W., Y.Z., J.L., J.C. and Y.H. analyzed the data and prepared the figures. S.J. wrote the original draft. S.J., D.W., S.W., C.P., J.C.

https://doi.org/10.1021/acs.nanolett.6c00074
Nano Lett. XXXX, XXX, XXX−XXX

and Y.H. revised the manuscript. All authors commented on the manuscript.

Funding

This work was financially supported by the National Key Research and Development Program of China (No. 2024YFB4610700), the National Natural Science Foundation of China (Nos. 52375582, 62575274, 62325507), the Fundamental Research Funds for the Central universities (WK2090000088, WK2090000081), Research Funds of Centre for Leading Medicine and Advanced Technologies of IHM (2025IHM01010).

Notes

The authors declare no competing financial interest.

■ ACKNOWLEDGMENTS

We acknowledge the Experimental Center of Engineering and Material Sciences at USTC for the fabrication and measuring of samples. This work was partly carried out at the USTC Center for Micro and Nanoscale Research and Fabrication.

■ REFERENCES

(1) Pipper, J.; Inoue, M.; Ng, L. F.-P.; Neuzil, P.; Zhang, Y.; Novak, L. Catching Bird Flu in a Droplet. *Nat. Med.* **2007**, *13* (10), 1259−1263.
(2) Marmottant, P.; Hilgenfeldt, S. Controlled Vesicle Deformation and Lysis by Single Oscillating Bubbles. *Nature* **2003**, *423* (6936), 153−156.
(3) Velev, O. D.; Prevo, B. G.; Bhatt, K. H. On-Chip Manipulation of Free Droplets. *Nature* **2003**, *426* (6966), 515−516.
(4) Li, W.; Tang, X.; Wang, L. Photopyroelectric Microfluidics. *Sci. Adv.* **2020**, *6* (38), No. eabc1693.
(5) Dai, H.; Dong, Z.; Jiang, L. Directional Liquid Dynamics of Interfaces with Superwettability. *Sci. Adv.* **2020**, *6* (37), No. eabb5528.
(6) Lin, F.; Wo, K.; Fan, X.; Wang, W.; Zou, J. Directional Transport of Underwater Bubbles on Solid Substrates: Principles and Applications. *ACS Appl. Mater. Interfaces* **2023**, *15* (8), 10325−10340.
(7) Zhou, Y.; Huang, S.; Tian, X. Magnetoresponsive Surfaces for Manipulation of Nonmagnetic Liquids: Design and Applications. *Adv. Funct. Mater.* **2020**, *30* (6), 1906507.
(8) Deng, Q.; Zhu, H.; Zhao, Z.; Li, H.; Yang, L.; Wu, X.; Zhang, Y.; Yu, P.; Tang, X.; Li, W.; Yin, X.; Wang, L. Linear Magnet with Fluid-Solid-Switchable Cells for Flexible Devices. *Nat. Commun.* **2025**, *16* (1), 4601.
(9) Deng, Q.; Li, H.; Zhu, H.; Yang, L.; Li, W.; Yin, X.; Zhang, Y.; Wang, L. Spatiotemporal Modulation of Magnetization in Magnetic Soft Materials. *Adv. Mater.* **2025**, *37* (48), No. e06342.
(10) Zhang, J.; Wang, X.; Wang, Z.; Pan, S.; Yi, B.; Ai, L.; Gao, J.; Mugele, F.; Yao, X. Wetting Ridge Assisted Programmed Magnetic Actuation of Droplets on Ferrofluid-Infused Surface. *Nat. Commun.* **2021**, *12* (1), 7136.
(11) Zhu, S.; Bian, Y.; Wu, T.; Chen, C.; Jiao, Y.; Jiang, Z.; Huang, Z.; Li, E.; Li, J.; Chu, J.; Hu, Y.; Wu, D.; Jiang, L. High Performance Bubble Manipulation on Ferrofluid-Infused Laser-Ablated Microstructured Surfaces. *Nano Lett.* **2020**, *20* (7), 5513−5521.
(12) Gunatilake, U. B.; Alvarez-Braña, Y.; Ojeda, E.; Basabe-Desmonts, L.; Benito-Lopez, F. Underwater Magneto-Driven Air de-Bubbler. *J. Mater. Chem. A* **2022**, *10* (24), 12832−12841.
(13) Li, A.; Li, H.; Li, Z.; Zhao, Z.; Li, K.; Li, M.; Song, Y. Programmable Droplet Manipulation by a Magnetic-Actuated Robot. *Sci. Adv.* **2020**, *6* (7), No. eaay5808.
(14) Chen, C.; Yao, H.; Jiao, Y.; Jia, C.; Wu, S. Magnetic-Actuated Robot Enables High-Performance Underwater Bubble Maneuvering on Laser-Textured Biomimetic Slippery Surfaces. *Langmuir* **2022**, *38* (6), 2174−2184.
(15) Jing, X.; Chen, H.; Zhang, L.; Zhao, S.; Wang, Y.; Wang, Z.; Zhou, Y. Accurate Magneto-Driven Multi-Dimensional Droplet Manipulation. *Adv. Funct. Mater.* **2023**, *33* (9), 2210883.
(16) Lin, Y.; Hu, Z.; Zhang, M.; Xu, T.; Feng, S.; Jiang, L.; Zheng, Y. Magnetically Induced Low Adhesive Direction of Nano/Micropillar Arrays for Microdroplet Transport. *Adv. Funct. Mater.* **2018**, *28* (49), 1800163.
(17) Ben, S.; Ning, Y.; Zhao, Z.; Li, Q.; Zhang, X.; Jiang, L.; Liu, K. Underwater Directional and Continuous Manipulation of Gas Bubbles on Superaerophobic Magnetically Responsive Microcilia Array. *Adv. Funct. Mater.* **2022**, *32* (28), 2113374.
(18) Han, K.; Yong, K. Overcoming Limitations in Surface Geometry-Driven Bubble Transport: Bidirectional and Unrestricted Movement of an Underwater Gas Bubble Using a Magnetocontrollable Nonwetting Surface. *Adv. Funct. Mater.* **2021**, *31* (26), 2101970.
(19) Liu, M.; Li, C.; Peng, Z.; Yao, Y.; Chen, S. A Mechanical Hand-like Functional Surface Capable of Efficiently Grasping and Non-Destructively Releasing Droplets. *Chem. Eng. J.* **2022**, *430*, 132749.
(20) Park, S.; Bang, J.; So, H. 3D Printing-Assisted and Magnetically-Actuated Superhydrophobic Surfaces for Droplet Control. *Surf. Interfaces* **2023**, *37*, 102678.
(21) Liu, H.; Zheng, S.; Yang, X.; Liao, W.; Wang, C.; Miao, W.; Tang, J.; Wang, D.; Tian, Y. Magnetic Actuation Multifunctional Platform Combining Microdroplets Delivery and Stirring. *ACS Appl. Mater. Interfaces* **2019**, *11* (50), 47642−47648.
(22) Yang, C.; Zhang, Z.; Li, G. Programmable Droplet Manipulation by Combining a Superhydrophobic Magnetic Film and an Electromagnetic Pillar Array. *Sens. Actuators, B* **2018**, *262*, 892−901.
(23) Nasirimarekani, V.; Benito-Lopez, F.; Basabe-Desmonts, L. Tunable Superparamagnetic Ring (tSPRing) for Droplet Manipulation. *Adv. Funct. Mater.* **2021**, *31* (32), 2100178.
(24) Demirörs, A. F.; Aykut, S.; Ganzeboom, S.; Meier, Y. A.; Poloni, E. Programmable Droplet Manipulation and Wetting with Soft Magnetic Carpets. *Proc. Natl. Acad. Sci. USA* **2021**, *118* (46), No. e2111291118.
(25) Dorvee, J. R.; Derfus, A. M.; Bhatia, S. N.; Sailor, M. J. Manipulation of Liquid Droplets Using Amphiphilic, Magnetic One-Dimensional Photonic Crystal Chaperones. *Nat. Mater.* **2004**, *3* (12), 896−899.
(26) Yang, X.; Shang, W.; Lu, H.; Liu, Y.; Yang, L.; Tan, R.; Wu, X.; Shen, Y. An Agglutinate Magnetic Spray Transforms Inanimate Objects into Millirobots for Biomedical Applications. *Sci. Robot.* **2020**, *5* (48), No. eabc8191.
(27) Liu, J. A.-C.; Gillen, J. H.; Mishra, S. R.; Evans, B. A.; Tracy, J. B. Photothermally and Magnetically Controlled Reconfiguration of Polymer Composites for Soft Robotics. *Sci. Adv.* **2019**, *5* (8), No. eaaw2897.
(28) Nieuwelink, A.-E.; Vollenbroek, J. C.; Tiggelaar, R. M.; Bomer, J. G.; van den Berg, A.; Odijk, M.; Weckhuysen, B. M. High-Throughput Activity Screening and Sorting of Single Catalyst Particles with a Droplet Microreactor Using Dielectrophoresis. *Nat. Catal.* **2021**, *4* (12), 1070−1079.
(29) Li, G.; Zhang, T.; Shen, Y. Transparent Magnetic Soft Millirobot Actuated by Micro-Node Array. *Adv. Mater. Technol.* **2021**, *6* (8), 2100131.
(30) Lathia, R.; Nagpal, S.; Modak, C. D.; Mishra, S.; Sharma, D.; Reddy, B. S.; Nukala, P.; Bhat, R.; Sen, P. Tunable Encapsulation of Sessile Droplets with Solid and Liquid Shells. *Nat. Commun.* **2023**, *14* (1), 6445.
(31) Wang, D.; Zhu, L.; Chen, J.-F.; Dai, L. Liquid Marbles Based on Magnetic Upconversion Nanoparticles as Magnetically and Optically Responsive Miniature Reactors for Photocatalysis and Photodynamic Therapy. *Angew. Chem.* **2016**, *128* (36), 10953−10957.
(32) Gach, P. C.; Sims, C. E.; Allbritton, N. L. Transparent Magnetic Photoresists for Bioanalytical Applications. *Biomaterials* **2010**, *31* (33), 8810−8817.
(33) Bshary, R.; Hohner, A.; Ait-el-Djoudi, K.; Fricke, H. Interspecific Communicative and Coordinated Hunting between

https://doi.org/10.1021/acs.nanolett.6c00074
Nano Lett. XXXX, XXX, XXX−XXX

Groupers and Giant Moray Eels in the Red Sea. *PLoS Biol.* **2006**, *4* (12), No. e431.
(34) Holldobler, B. K.; Wilson, E. O. Weaver Ants. *Sci. Am.* **1977**, *237*, 146−155.
(35) Wang, Y.; Zhang, L.; Du, W.; Zhou, X.; Guo, Y.; Zhao, S.; Liu, G.; Zhang, D.; Chen, H. Controllable Bubble Transport on Bioinspired Heteromorphic Magnetically Steerable Microcilia. *Adv. Funct. Mater.* **2023**, *33* (35), 2302666.
(36) Feng, W.; Ueda, E.; Levkin, P. A. Droplet Microarrays: From Surface Patterning to High-Throughput Applications. *Adv. Mater.* **2018**, *30* (20), 1706111.
(37) Jiao, L.; Wu, Y.; Hu, Y.; Guo, Q.; Wu, H.; Yu, H.; Deng, L.; Li, D.; Li, L. Mosaic Patterned Surfaces toward Generating Hardly-Volatile Capsular Droplet Arrays for High-Precision Droplet-Based Storage and Detection. *Small* **2023**, *19* (14), 2206274.
(38) Guo, X.; Li, H.; Yeop Ahn, B.; Duoss, E. B.; Hsia, K. J.; Lewis, J. A.; Nuzzo, R. G. Two- and Three-Dimensional Folding of Thin Film Single-Crystalline Silicon for Photovoltaic Power Applications. *Proc. Natl. Acad. Sci. U.S.A.* **2009**, *106* (48), 20149−20154.
(39) Py, C.; Reverdy, P.; Doppler, L.; Bico, J.; Roman, B.; Baroud, C. N. Capillary Origami: Spontaneous Wrapping of a Droplet with an Elastic Sheet. *Phys. Rev. Lett.* **2007**, *98* (15), 156103.
(40) Jiang, S.; Li, B.; Zhao, J.; Wu, D.; Zhang, Y.; Zhao, Z.; Zhang, Y.; Yu, H.; Shao, K.; Zhang, C.; Li, R.; Chen, C.; Shen, Z.; Hu, J.; Dong, B.; Zhu, L.; Li, J.; Wang, L.; Chu, J.; Hu, Y. Magnetic Janus Origami Robot for Cross-Scale Droplet Omni-Manipulation. *Nat. Commun.* **2023**, *14* (1), 5455.
(41) Kim, Y.; Zhao, X. Magnetic Soft Materials and Robots. *Chem. Rev.* **2022**, *122* (5), 5317−5364.
(42) Yang, X.; Tan, R.; Lu, H.; Fukuda, T.; Shen, Y. Milli-Scale Cellular Robots That Can Reconfigure Morphologies and Behaviors Simultaneously. *Nat. Commun.* **2022**, *13* (1), 4156.
(43) Low, L. A.; Mummery, C.; Berridge, B. R.; Austin, C. P.; Tagle, D. A. Organs-on-Chips: Into the next Decade. *Nat. Rev. Drug Discovery* **2021**, *20* (5), 345−361.
(44) Yu, C.; Zhang, P.; Wang, J.; Jiang, L. Superwettability of Gas Bubbles and Its Application: From Bioinspiration to Advanced Materials. *Adv. Mater.* **2017**, *29* (45), 1703053.
(45) Shao, K.; Jiang, S.; Hu, Y.; Zhang, Y.; Li, C.; Zhang, Y.; Li, J.; Wu, D.; Chu, J. Bioinspired Lubricated Slippery Magnetic Responsive Microplate Array for High Performance Multi-Substance Transport. *Adv. Funct. Mater.* **2022**, *32* (40), 2205831.
(46) Bhosale, P. S.; Panchagnula, M. V.; Stretz, H. A. Mechanically Robust Nanoparticle Stabilized Transparent Liquid Marbles. *Appl. Phys. Lett.* **2008**, *93* (3), 034109.
(47) Barrera, N. M.; McCarty, J. L.; Dragojlovic, V. Effects of Concentration on Hexaaquacobalt(II)/Tetrachlorocobalt(II) Equilibrium. A Discovery-Oriented Experiment for Chemistry Students. *Chem. Educ.* **2002**, *7* (3), 142−145.
(48) Li, J.; Mooney, D. J. Designing Hydrogels for Controlled Drug Delivery. *Nat. Rev. Mater.* **2016**, *1* (12), 16071.
(49) Ding, S.; Duan, S.; Chen, Y.; Xie, J.; Tian, J.; Li, Y.; Wang, H. Centrifugal Microfluidic Platform with Digital Image Analysis for Parallel Red Cell Antigen Typing. *Talanta* **2023**, *252*, 123856.

https://doi.org/10.1021/acs.nanolett.6c00074
Nano Lett. XXXX, XXX, XXX−XXX